Packaged connecting-slab grating under the second Bragg incidence for three-port splitting

JIMIN FANG, BO WANG*, CHENHAO GAO, CHEN FU, KUNHUA WEN, ZIMING MENG, ZHAOGANG NIE*, XIANGJUN XING, LI CHEN, LIANG LEI, JINYUN ZHOU
School of Physics and Optoelectronic Engineering, Guangdong University of Technology, Guangzhou 510006, China

The three-port grating with a connecting slab under the second Bragg incidence is introduced in this paper. In order to improve bandwidth, in the case of a given duty cycle of 0.6, grating structure is described so that the three grating diffraction orders are with efficiencies over 30%, where bandwidths are 91 nm and 24 nm for TE and TM polarizations, respectively. For the optimized optimal solution, we can use the modal method to explain the physical process of grating diffraction.

(Received March 21, 2019; accepted April 9, 2020)

Keywords: Polarization-dependent grating, Beam splitters, The second Bragg incidence

1. Introduction

The polarization-dependent microstructures [1-4] can be used as elements. And beam splitters [5-8] are presented in order to achieve efficient transmission efficiency and good beam splitting effect. The beam splitter divides the incident light into several directions [9-13]. Micro-gratings have been proposed for various applications in optical systems [14-20]. Under the second Bragg incidence, grating energy is mainly divided into the -2nd order and the -1st order and the 0th order. The efficiency of the three diffraction orders is close to 33% and three-port gratings are widely used in interferometers [21,22] and holographic applications [23]. Li *et al.* [24] designed the fused-silica sandwiched three-port grating. Compared with the Ref. [24], our designed gratings have lower overall efficiency owing to energy loss, but we can see that the bandwidth optimization result is better than that in the reported Ref. [24].

The research method of the three-port grating is rigorous coupled-wave analysis (RCWA) method [25] and modal method [26]. We analyze the incident light, the mode of propagation and diffraction orders by modal method, revealing the physical process of grating diffraction. And the method of grating diffraction can guide the design of deep-etched gratings. In addition to this design, in order to meet the requirements of cleaning and protecting the device in practical applications, a covering layer is added. This design adds a covering layer, which not only enriches the type of three-port beam splitter, but also increases the period and bandwidth tolerance of the grating.

In this paper, a three-port grating beam splitter with a connecting slab under the second Bragg incidence is designed. The grating structure includes a covering layer, a grating layer with a connecting slab, and a substrate. By using the RCWA method, we get the optimized parameters of the grating beam splitter. For TE-polarized light, the efficiencies in the 0th order, -1st order and the -2nd order can reach 32.58%, 32.45% and 32.49%. For TM-polarized light, the efficiencies of three orders are 31.28%, 31.01% and 31.60%. And the bandwidth is better than the previous result.

2. Modal analysis and numerical design

Fig. 1 depicts the three-port grating beam splitter with a connecting slab under the second Bragg incidence, from the top to the bottom of the grating, the grating is divided into a covering layer, a grating layer, and a substrate layer. The first part has a refractive index of n_2=1.45, and the second part is a grating ridge and a connecting slab, and the material is fused silica. Fused silica has high transmission efficiency [27-29] and can work under high intensity laser conditions [30-32]. The grating groove medium is air with a refractive index n_1=1.0. The duty cycle is a fixed value, and we set it to 0.6. The third part is the grating substrate made of Ta_2O_5 with n_3=2.0. In addition, the grating period can be expressed as d_{TE} under TE-polarized light and d_{TM} under TM-polarization.

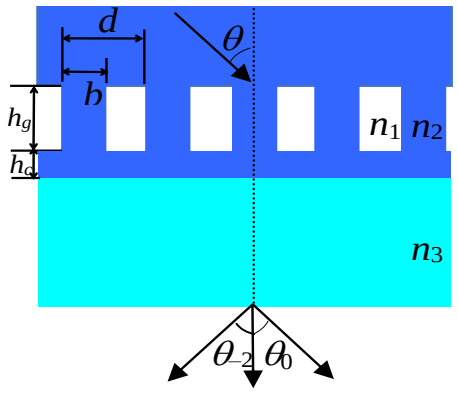

Fig. 1. (Color online) Structure diagram of fused-silica grating with a connecting slab under the second Bragg angle

For this grating structure, we design d_{TE}=1060 nm and d_{TM}=1137 nm. The depth of the grating groove can be expressed as h_{gTE} of TE-polarization or h_{gTM} of TM-polarized light. Symbol h_{cTM} or h_{cTE} can represent the thickness of the connecting slab. λ is equivalent to 800 nm wavelength. The angle of incidence is $\theta=\sin^{-1}(\lambda/n_2 d)$. In this case, the grating period of d is in the range of λ-2λ, and three diffraction orders are excited and generated on the grating substrate. Fig. 2 shows the relationship of three diffraction efficiency ratios with depth h_g and the connection layer thickness h_c at a wavelength of 800 nm under the second Bragg incidence. As can be seen from Fig. 2, the ratio of the -1st order to the 0th order efficiency is 0.996, and the ratio of the -2nd to -1st order is 1.001 in the case of d_{TE}=1060 nm, h_{gTE}=0.87 μm and h_{cTE}=0.16 μm. The efficiency is 32.58%, 32.45% and 32.49%. At a 1137 nm period of TM polarization, grating groove depth is 1.25 μm and connecting slab thickness is 2.30 μm. The efficiency ratio of the -1st order to the 0th order is near 0.9912, the ratio of the -2nd to -1st order is 1.019, and the TM polarization efficiency is 31.28%, 31.01% and 31.60%.

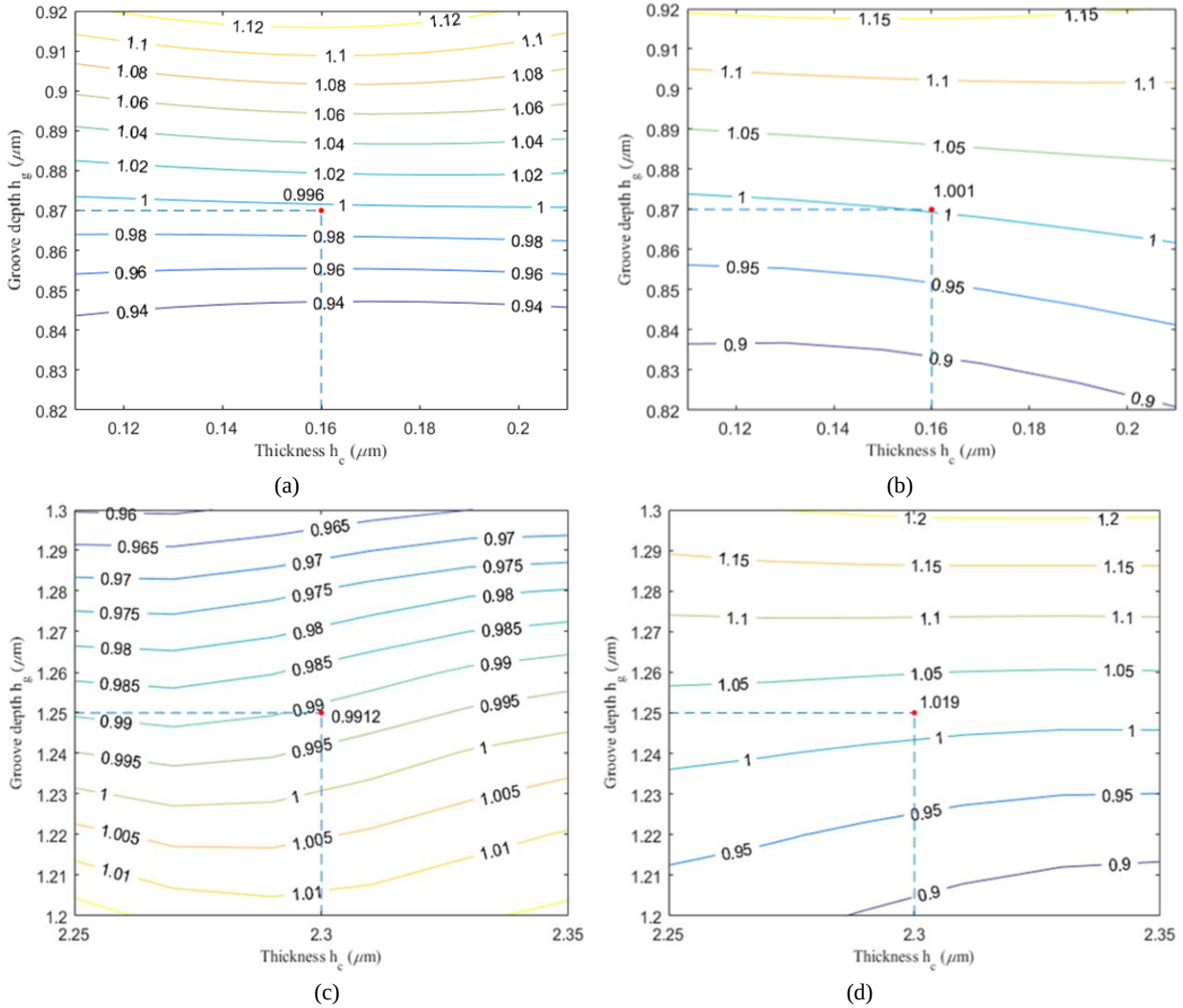

Fig. 2. (Color online) Diffraction efficiency's ratios of the -1st order to the 0th order and the -2nd order to the -1st order versus the grating groove depth and the depth of connection layer: (a) efficiency's ratio of the -1st order and the 0th order for TE polarization, (b) efficiency's ratio of the -2nd order and the -1st order for TE polarization, (c) efficiency's ratio of the -1st order and the 0th order for TM polarization, (d) efficiency's ratio of the -2nd order and the -1st order for TM polarization

Table 1. Coupling overlap integration between three grating modes and three diffraction orders of an optimized grating parameter at an incident wavelength of 800 nm: (a) TE polarization and (b) TM polarization

Mode → Orders	-2nd	-1st	0th
(a)			
Modes 0	0.10358	0.79240	0.10358
Modes 1	0.48069	0	0.48069
Modes 2	0.37669	0.19492	0.37669
(b)			
Modes 0	0.15541	0.68439	0.15541
Modes 1	0.44847	0	0.44847
Modes 2	0.36194	0.18984	0.36194

For diffraction behavior of TE-polarized light and TM-polarized light with an incident wavelength of 800 nm and a duty cycle of 0.6, the effective refractive index values of the three diffraction orders are respectively:

$$n_{0,eff}^{TE}=1.3810, n_{1,eff}^{TE}=1.1323, n_{2,eff}^{TE}=0.9048,$$
$$n_{0,eff}^{TM}=1.3653, n_{1,eff}^{TM}=1.0941, n_{2,eff}^{TM}=0.9661.$$

Based on the optimized grating parameters, we use the modal method to explain the diffraction phenomenon of the grating under the quadratic Bragg incidence. We ignore the reflection of the grating mode at different media interfaces, only considering modes [33,34] in which the light is excited when it enters the grating. Energies are transmitted during coupling [35]. Considering the energy coupling exchange between the grating mode and the diffraction order, the energy exchange capability can be proposed by the Table 1. The incident light excites three modes, which can get energies from the incident wave. Then, each mode will couple the energy into diffracted three orders by the overlap integration. Finally, transmission efficiencies are formed based on the coupling.

3. Results and discussion

In practical applications, the grating period may be deviated in the etching process. Fig. 3 considers the relationship between diffraction efficiency and the grating period. As shown in Fig. 3, TE polarization has a diffraction order efficiency greater than 30%, when the grating period tolerance range is 1007-1094 nm. In addition, for TM polarization light, efficiencies in the three orders are more than 30%, when the period tolerance is within the range of 1112-1151 nm. The grating has a large tolerance of period under TE polarization.

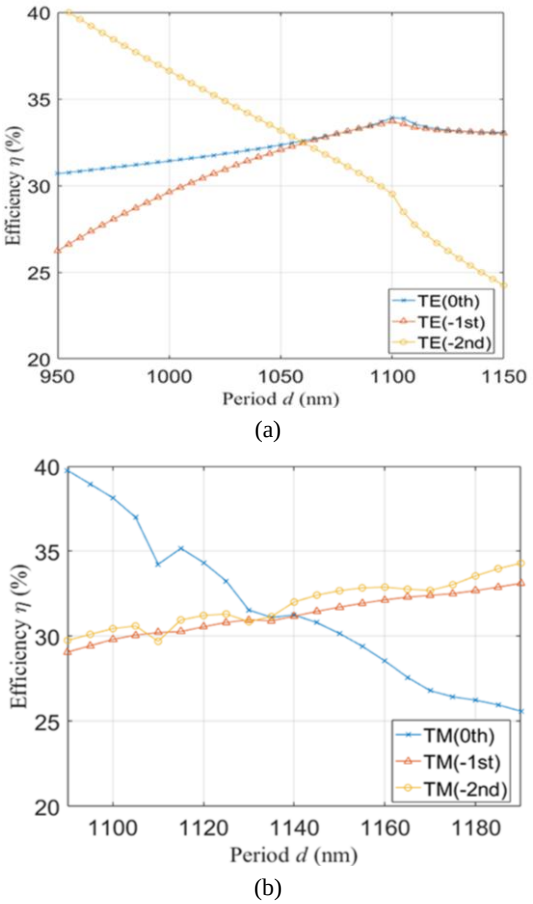

Fig. 3. (Color online) Diffraction efficiency versus the period for a wavelength of 800 nm under second Bragg angle: (a) TE polarization, (b) TM polarization

When the incident condition deviates from the optimized result, the performance is affected. Therefore, it is necessary to study the influence of the manufacturing tolerance of the variation of the incident wavelength and angle on the diffraction efficiency. Fig. 4 analyzes the change of grating efficiency in the wavelength range from 740 nm to 860 nm. As shown in Fig. 4, three diffraction orders efficiency of TE polarization are greater than 30%, when the wavelength range is 764-855 nm. The incident bandwidth is 91 nm for TE polarization. For comparison, 83 nm bandwidth is exhibited in Ref. [24]. In addition, for TM polarization light, efficiencies in the three orders are more than 30%, when the length of the incident light is within the range of 793-817 nm. The grating has a bandwidth of 24 nm for TM polarization. In Ref. [24], the bandwidth is 22 nm.

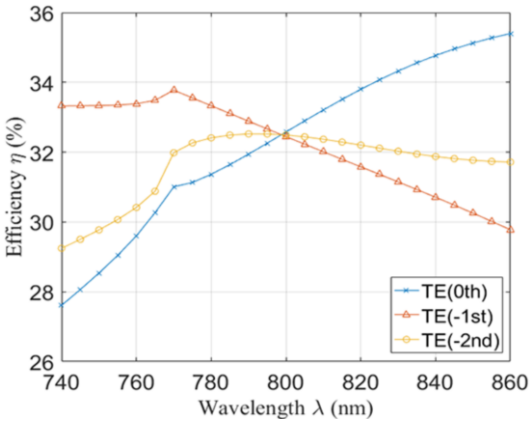

(a)

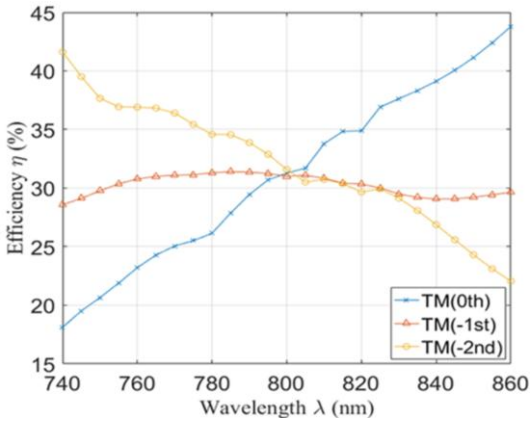

(b)

Fig. 4. (Color online) The efficiency corresponding to the incident wavelength for (a) TE polarization and (b) TM polarization

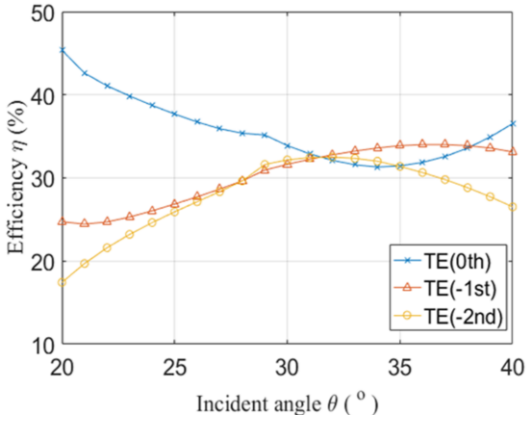

(a)

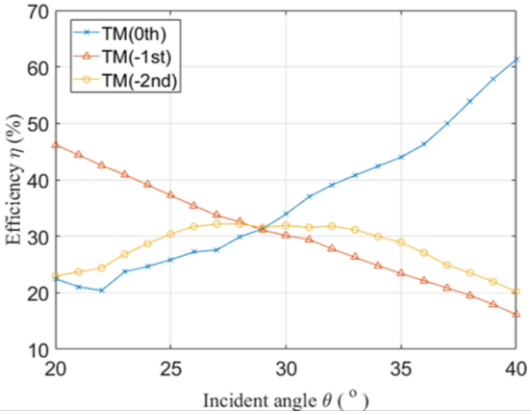

(b)

Fig. 5. (Color online) The diffraction efficiency corresponding to the incident angle near second Bragg condition: (a) TE polarization, (b) TM polarization

The incident angle bandwidth is also one of the parameters affecting the grating beam splitting structure. Fig. 5 reflects the relationship between the transmission efficiency of three orders and the incident angle of incident light. The abscissa is the incident angle and the ordinate is the transmission efficiency of each order. Efficiency is greater than 30% in the range of 28.3° -36.7° for TE polarized light. The angular bandwidth is 8.4°. Efficiency is greater than 30% in the incident angle bandwidth range of 28.1°-30.1° for TM polarized light. The angular bandwidth is 2.0°. TE polarized wave has a large incident angle bandwidth.

4. Conclusion

In this paper, we introduce a transmissive packaged three-channel grating beam splitter with a connection layer. This grating beam splitter is different from the previous literature in adding a connecting layer. To achieve a good beam splitting effect and increase the bandwidth, for TE polarized light, the diffraction efficiencies of the 0th, -1st and -2nd orders are 32.58%, 32.45% and 32.49%. For TM polarized light, the diffraction efficiencies of the diffraction wave of the 0th, -1st and -2nd orders are 31.28%, 31.01% and 31.6%. Based on the formation of the structural parameters, the incident wavelength and the incident angle bandwidths of the grating are analyzed. The results show that the wavelength bandwidth of the incident light of the TE polarization is better than the bandwidth of the incident light of the TM polarization in terms of the incident bandwidth.

Acknowledgements

This work is supported by the National Natural Science Foundation of China (11774071, 61675050, 11774069).

References

[1] B.-X. Wang, Q. Xie, G. Dong, W.-Q. Huang, Superlattice Microstruct. **114**, 225 (2018).
[2] S. Yin, B. Wang, C. Su, W. Zhu, L. Chen, L. Lei, J. Zhou, Optoelectron. Adv. Mat. **12**(5-6), 279 (2018).
[3] K. Jatiyanon, B. Soodchomshom, Superlattice Microstruct. **120**, 540 (2018).
[4] X. Shi, H. Long, J. Wu, L. Chen, L. Ying, Z. Zheng, B. Zhang, Superlattice Microstruct. **128**, 151 (2018).
[5] C. -C. Huang, Sci. Rep. **8**(1), 11 (2018).
[6] J. Xiao, Z. Guo, IEEE Photon. Technol. Lett. **30**(6), 529 (2018).
[7] J. Zhou, J. Wang, K. Guo, F. Shen, Q. Zhou, Z. Yin, Z. Guo, Superlattice Microstruct. **114**, 75 (2018).
[8] W. Fang, X. Fan, X. Zhang, H. Niu, H. Xu, J. Fei, Y. Huang, C. Bai, IEEE Photon. Technol. Lett. **30**(8), 708 (2018).
[9] A. Fedaouche, H. A. Badaoui, M. Abri, Optik **157**, 1300 (2018).
[10] Q. Zhang, M. Li, T. Liao, X. Cui, Opt. Commun. **411**, 93 (2018).
[11] Y.-Y. Fei, X.-D. Meng, M. Gao, Z. Ma, H. Wang, Optik **170**, 368 (2018).
[12] E. Rafiee, F. Emami, R. Negahdari, Optik **172**, 234 (2018).
[13] S. lv, J. Jing, Opt. Commun. **424**, 63 (2018).
[14] G. Zhou, W. Tian, Optik **172**, 1104 (2018).
[15] Y. Dai, H. Xu, H. Wang, Y. Lu, P. Wang, Opt. Commun. **416**, 66 (2018).
[16] T. Sharma, H. Kwon, J. Park, S. Han, G. Son, Y. Jung, K. Yu, Opt. Commun. **427**, 452 (2018).
[17] M. Gambhir, S. Gupta, Optik **164**, 567 (2018).
[18] M. Abolhassani, Optik **174**, 425 (2018).
[19] B. Zhang, Y. Liu, Z. Zhao, P. Yan, Opt. Commun. **427**, 448 (2018).
[20] J. Lu, B. Ding, Y. Huo, T. Ning, Opt. Commun. **415**, 146 (2018).
[21] Q. Lv, Z. Liu, W. Wang, X. Li, S. Li, Y. Song, H. Yu, Bayanheshig, W. Li, Appl. Opt. **57**(31), 9455 (2018).
[22] C. Lin, S. Yan, D. Ding, G. Wang, Opt. Eng. **57**(6), 064102 (2018).
[23] Z. Diao, L. Kong, J. Yan, J. Guo, X. Liu, L. Xuan, L. Yu, Chin. Opt. Lett. **17**(1), 012301 (2019).
[24] H. Li, B. Wang, H. Pei, L. Chen, L. Lei, J. Zhou, Superlattice Microstruct. **93**, 157 (2016).
[25] M. G. Moharam, D. A. Pommet, E. B. Grann, T. K. Gaylord, J. Opt. Soc. Am. A **12**(5), 1077 (1995).
[26] I. C. Botten, M. S. Craig, R. C. Mcphedran, J. L. Adams, J. R. Andrewartha, Opt. Acta **28**(3), 413 (1981).
[27] L. Tian, Y. Sun, Y. Cao, Y. Yi, F. Wang, Y. Wu, D. Zhang, IEEE Photon. Technol. Lett. **30**(7), 603 (2018).
[28] S. Ye, B. Wu, Z. Wang, C. Sun, B. Wei, C. Dong, S. Jian, IEEE Photon. J. **11**(1), 4800413 (2019).
[29] J.-S. Choe, H. Ko, B.-S. Choi, K.-J. Kim ; C. J. Youn, IEEE Photon. J. **10**(1), 7600108 (2018).
[30] M. S. Astapovich, A. V. Gladyshev, M. M. Khudyakov, A. F. Kosolapov, M. E. Likhachev, I. A. Bufetov, IEEE Photon. Technol. Lett. **31**(1), 78 (2019).
[31] L. Sun, R. Ni, H. Xia, T. Shao, J. Huang. X. Ye, X. Jiang, L. Cao, IEEE Photon. J. **10**(5), 8300115 (2018).
[32] J. Ascorbe, L. Coelho, J. L. Santos, O. Frazão, J. M. Corres, IEEE Photon. Technol. Lett. **30**(1), 67 (2018).
[33] C. Gao, B. Wang, H. Li, K. Wen, Z. Meng, Q. Wang, X. Xing, L. Chen, L. Lei, J. Zhou, Mod. Phys. Lett. B **32**(4), 1850042 (2018).
[34] H. Pei, B. Wang, W. Zhu, S. Yin, L. Chen, L. Lei, J. Zhou, Mod. Phys. Lett. B **32**(31), 1850386 (2018).
[35] B. Fang, L. Chen, X. Jing, Optik **171**, 130 (2018).

*Corresponding author: wangb_wsx@yeah.net
zgniegdut@163.com